ELSEVIER

Carbohydrate Research 266 (1995) 115–128

CARBOHYDRATE RESEARCH

Structural properties of native and sonicated cinerean, a β-(1→3)(1→6)-D-glucan produced by *Botrytis cinerea*

K.-Peter Stahmann [a,*], Nicole Monschau [a], Hermann Sahm [a], Anja Koschel [b], Michael Gawronski [b], Harald Conrad [b], Tasso Springer [b], Friedrich Kopp [c]

[a] *Institut für Biotechnologie 1, D-52425 Jülich, Germany*

[b] *Institut für Festkörperforschung, Forschungszentrum Jülich GmbH, D-52425 Jülich, Germany*

[c] *Diabetes Forschungsinstitut, Auf dem Hennekamp 65, D-40225 Düsseldorf, Germany*

Received 25 April 1994; accepted 5 July 1994

Abstract

Cinerean, the extracellular β-(1→3)(1→6)-D-glucan of the fungus *Botrytis cinerea* was studied. Electron micrographs of the native polysaccharide revealed quasi-endless fibrils with an estimated diameter of ca. 1.5 nm. A particle mass of 10^9–10^{10} daltons was determined from dilute solutions by low-angle laser light scattering. Sonication of increasing duration led to fragmentation of the native polymer with an approximately exponential decrease of mass in the range of average molecular masses between 250 000 and 50 000 daltons. Shadowed by platinum, cinerean fibril fragments with a weight-average molecular mass of 172 000 ± 3000 daltons could be characterized from electron micrographs as a distribution of rods of most probable length of 45 nm and an average length of 72 nm. Small-angle X-ray scattering confirmed the fibrillar structure of the native cinerean and the rodlike structure of sonicated cinerean. A rod diameter of 1.9 ± 0.2 nm and a mass per unit length of 2250 ± 490 daltons/nm were found. The latter is in agreement with the value of 1830 daltons/nm calculated from the length distribution determined from the electron micrographs. These data – especially the mass per unit length – suggest a quaternary structure for the polysaccharide. Such a structure would explain the rigidity of the rods which, in turn, is responsible for the characteristic phase separation behaviour in aqueous solutions observed by nephelometry and viscometry.

Keywords: Polysaccharide; Cinerean; Rigid rods; Phase separation; Sonication

1. Introduction

The significance of fungal glucans, such as krestin, lentinan, schizophyllan, or scleroglucan as unspecific modulators of the immune system, e.g., for adjuvant application against

* Corresponding author.

SSDI 0008-6215(94)00245-2

tumours, has been increasing in recent years. In 1985, krestin reached rank nineteen in the list of the most frequently sold pharmaceuticals in the world with an annual turnover of 255 million dollars [1]. One method of understanding and optimizing the physiological effect is the systematic comparison of a great number of substances varying slightly in their structure. A less studied variant is formed by the ascomycete *Botrytis cinerea*. This fungus produces an extracellular β-(1→3)(1→6)-D-glucan (cinerean) during growth in mineral salts medium with D-glucose as the sole carbon source [2]. The polymer forms a capsule strongly adhering to the hyphae and can be used by the fungus as a carbon and energy store [3]. The relatively well-known biological response modifiers lentinan, scleroglucan, and schizophyllan have been found to form triple helices of remarkably high rigidity [4,5] in native as well as sonicated specimens. Biochemical and physical studies were performed in order to characterize cinerean and compare it to the glucans just mentioned.

From a physical point of view, sufficiently long, rigid molecules are interesting as they tend to form ordered structures in solutions (so-called lyotropic liquid crystals [6]) even without attractive intermolecular interactions [7]. The type of structure actually obtained may nevertheless involve much more complicated interactions. The investigation of these interactions is not only of academic interest, as demonstrated by many technological developments of high performance fibers like KEVLAR [1] composed of the stiff chain aromatic polyamide poly(*p*-phenylene terephthalamide) [8]. For example, the very existence of nematic order (i.e., axial alignment of elongated molecules) in solution is the clue to understanding the microscopic structure and rigidity of the jet-spun fibers from solution. In fact, X-ray diffraction has revealed a high degree of axial alignment of the individual rodlike polymer molecules in the fibers as well [9].

Most remarkably, only sonicated cinerean solutions revealed ordered structures as described above. On the other hand, the quaternary structure responsible for the rigidity seems to be important for physiological activity [10], and the availability of cinerean fragments was desirable because even lentinan fragments with average molecular weights of 6×10^3 showed antitumour effects [11].

2. Experimental

β-D-Glucan formation.—The polymer was produced by the cultivation of *Botrytis cinerea* strain LU 1478 MaB in a mineral salts medium with *D*-glucose (20 g/L) as the sole carbon source and KNO_3 (1.5 g/L) as the sole nitrogen source. Cultivation conditions and precipitation of the extracellular polysaccharide have been described elsewhere [3].

Enzymatic degradation.—Cinerean used for total hydrolysis was labeled by feeding the culture with D-[U-^{14}C]glucose. After degradation of the polymer by Novozym^{R} SP-116 (Novo-Industries, Denmark), the starting material and product were separated by thin layer chromatography (TLC) [12]. Detection and quantification were performed with an automatic TLC linear analyzer (type LB2821, Berthold, Germany). For specific hydrolysis of the β-(1→3) linkages, glucanase II, an enzyme purified from the culture supernatant of *B.*

[1] KEVLAR is a registered trademark for amide fibers by DuPont.

Table 1
Conditions of cinerean sonication

Applied sample	Volume (mL)	Cinerean (g/L)	Intensity	Duration (h)	M_w by LALLS [a]
Native cinerean	116	15	2	38	249 000
249 000 fragment	15	15	2	5.5	165 000
249 000 fragment	15	15	2	11	148 000
249 000 fragment	15	15	2	26.5	52 000
Native cinerean	100	30	5	3.5	
			10	10.5	172 000

[a] M_w, molecular weight; LALLS, low-angle laser light scattering.

cinerea [13], was used and the degradation products were separated and quantified in the form of their borate complexes by anion-exchange chromatography [3].

Ultrasonic irradiation.—Sonication was performed with a Branson B-15 P instrument. Table 1 shows the conditions leading to the cinerean fragments studied. To avoid heating, the samples were cooled by an ice bath during sonication. Metal fragments from the standard 1/2″ horn of the sonifier were removed by centrifugation for 20 min at 4000*g*. The cinerean fragments were precipitated from the solution by adding 2-propanol (2 vol). After centrifugation at 4000*g*, the pellet was dried overnight at 60°C.

Gel filtration chromatography.—A column 2.5 cm in diameter, packed with 99.5 cm of Fractogel TSK HW 55 (S) and a top layer (11.5 cm) of Fractogel TSK HW 65 (S) was equilibrated with 50 mM NaOAc buffer containing 0.3 M NaCl at pH 5.0. To minimize unwanted interactions, the system was run at 40°C. A volume of 5 mL containing 12 mg sample was applied. Flow was kept constant at 21.2 mL/h and fractions were collected every 15 min. The saccharide content in the fractions was determined with anthrone [14].

Electron microscopy.—For negative staining of the purified native glucan, a 10-μL droplet of distilled water containing 20 μg glucan per mL was applied to a carbon-coated Formar grid that had been rendered hydrophilic by a 30-s exposure to a glow discharge in a plasma cleaner (Harrick Scientific Corporation, New York). After adsorption for 35 min, the droplet was removed with a strip of filter paper and 10 μL of aq 2% uranyl acetate was applied to the grid. After 1 min, most of the stain was removed and the grid was dried.

For preparation of heavy-metal-shadowed specimens of sonicated glucan molecules, a 10-μL droplet containing 20 μg glucan per mL was allowed to adsorb onto a small piece of freshly cleaved mica for 1 min. The adhering solution was removed from the edge of the piece of mica with a glass capillary. While still covered with a film of moisture, the specimen was frozen by plunging into liquid nitrogen. The frozen sample was positioned in a closed holder on the rotatable cool table of a BALZERS freeze-etch device BAF 400 D equipped with a liquid-nitrogen-cooled Meissner trap, exposed to a vacuum better than 10^{-7} mbar, and freeze dried at −80°C. When all remnants of ice had disappeared (after ca. 30 min), the sample was conically coated with platinum under an angle of 10°. The amount of platinum deposited was measured with a quartz crystal film-thickness monitor. It was found to be close to 0.1 nm relative to the plane of the substrate. To reinforce the replica, an additional 20 nm of carbon was evaporated vertically onto the object plane. The replicas were floated onto a swept water surface and picked up onto Forvar-coated EM grids.

Cleaning of the replicas was found to be unnecessary. The samples were viewed with a Siemens Elmiskop 102 calibrated with a muscovite.

Low-angle laser light scattering (LALLS).—Weight-average molecular masses $\overline{M}_W$ of native and sonicated cinerean were determined on an absolute scale with the LALLS Photometer KMX-6 from LDC Analytical. In order to eliminate contributions from higher order terms A_n of the virial expansion, measurements of a series of low concentrations ($c \leq 4 \times 10^{-5}$ g/cm^3) of aqueous cinerean solutions were performed, the molecular mass was finally determined from an extrapolation to zero concentration, and the zero scattering angle θ was calculated according to the expression [15]

$$\frac{cK}{\Delta R_\theta} = \frac{1}{\overline{M_W} \cdot P(\theta)} + 2A_2 c \tag{1}$$

where ΔR_θ is the difference in Rayleigh ratios of solution and solvent, $P(\theta)$ the normalized molecular form factor, and $K = \text{const} \cdot (dn/dc)^2|_{c=0}$ is the contrast factor. The refractive index increment dn/dc was determined with the Differential Refractometer KMX-16 from LDC Analytical.

Nephelometry.—The reversible turbidity of the cinerean solutions resulting from the formation and decay of polymer clusters when passing the solubility limits was observed with a laser light transmission apparatus developed in our laboratory. The laser light transmitted through a temperature-controlled quartz vessel containing the sample was measured by a photo diode and recorded with an *X–Y*-plotter together with the output of a thermocouple placed inside the cinerean solutions. The temperature-controlled vessel was mounted in a container filled with dry Ar to prevent condensation of air moisture on the quartz windows when measuring at temperatures below the dew point.

Viscometry.—Viscosities of the sonicated cinerean solutions were determined with the automatic viscosity measuring apparatus AVS 310 from Schott-Geräte GmbH. The Ubbelohde capillary viscosimeter from Schott-Geräte was placed in a thermostat (CT 1450 from Schott-Geräte) filled with a water–glycol mixture, the temperature of which was controlled to ± 0.01°C. Kinematic viscosities ν are directly proportional to the efflux time t according to $\nu = K \cdot t$ (Hagen–Poiseuille law), the exact value of K to be determined by a calibration run with a substance of known viscosity. Because we were only interested in changes of viscosities as a function of solution temperature or composition we used the K-value given by the manufacturer, i.e., $K = 0.9482$ for a capillary of 12-cm length and a diameter of 1.26 mm.

X-ray small-angle scattering.—The scattering measurements were carried out employing both the 100-kW rotating anode X-ray small-angle instrument and the equivalent synchrotron radiation facility JUSIFA [16] installed at the DORIS storage ring at DESY, Hamburg. Both installations use two-dimensional position-sensitive detectors that greatly improves the statistical accuracy of the data at large scattering angles. The primary X-ray energies used were the 8-keV Cu$K\alpha$ radiation with the rotating anode machine and correspondingly 8 and 14 keV with synchrotron radiation. All data were calibrated using amorphous carbon as the standard scatterer so as to obtain molecular masses in absolute units.

3. Results and discussion

Polysaccharide composition and linkages.—Cinerean is a homopolymer of D-glucose [2,17,18]. The samples used in our experiments were degraded by Novozym^R, an enzyme

preparation which cleaves all glycosidic linkages of the polysaccharide. Only glucose was found by borate-complex anion-exchange chromatography. For a total recovery of applied cinerean and liberated glucose, ^{14}C-labelled cinerean was digested and analyzed by TLC. As much as 96% was detected as glucose and only 4% remained undegraded at the starting point. This confirms that in mineral salts medium with a high C:N ratio and D-glucose as the sole carbon source, the reported heteropolysaccharide [19] is not produced. Cinerean consists of a β-(1→3)-linked backbone with branches of β-(1→6)-linked single glucosyl groups [2,18]. The degree of branching was analyzed with a specific β-(1→3)-D-glucanase. Because this enzyme cleaves only the β-(1→3) linkages of the polymer, each liberated molecule of gentiobiose, the β-(1→6)-linked glucose dimer, means a branchpoint, while each glucose molecule split off from the polymer represents an unbranched part of the chain. For cinerean, a glucose–gentiobiose ratio of 1.38 ± 0.07 was found. This property may differ with the fungal strain and culture conditions because ratios of 1.9 [17] and 0.7 [2,18] have been reported. In parallel experiments, scleroglucan (1.53 ± 0.08) and schizophyllan (1.67 ± 0.07) were found to have a lower degree of branching. The structure and the sizes of a statistically branched segment of cinerean are shown in Fig. 1.

Molecular mass of native cinerean.—The molecular mass of cinerean was found to be much higher than that described in the literature. A sample applied to a gel filtration column packed with Fractogel TSK HW 65(S) was eluted before the 2 000 000 daltons dextran standard. Because no standards above 2 000 000 are available, low-angle laser light scattering was performed. Molecular weights of 5×10^9 and 2×10^{10} were determined in two independent measurements. This result is 3–4 orders of magnitude higher than the masses reported for determinations by viscometry [20] and ultracentrifugation [18]. The spatial extension of the individual cinerean threads was estimated from the pronounced angular dependence $P(\theta)$ (compare Eq. 1) of the scattered light observed between 2 and 7° (the range accessible with the KMX-6). An rms end-to-end distance $\sqrt{\overline{h^2}}$ of 2 μm was determined. This result clearly shows a very compact conformation of native cinerean as compared to the length of an extended chain of similar mass. The critical concentration for nonoverlapping solute particles estimated from $\sqrt{\overline{h^2}}$ gave $c_{crit} = 0.87$ mg/mL, a value greatly exceeding the highest concentration used. Actually, several series of dilutions between 5 and 40 μg/mL were measured and the apparent molecular weights extrapolated to zero concentration. For concentrations much below the critical, such an extrapolation is expected to give reliable figures for the particle masses, although stable molecular aggregations cannot be ruled out in principle by this technique. The influence of shear stress during cultivation of the fungus was not studied. This is a possible reason for the discrepancy from the literature values.

Conformation of the native polymer.—An amorphous structure of a powder sample was found by X-ray diffraction and electron microscopy for cinerean [2]. On the other hand, it is now accepted that scleroglucan and schizophyllan form rodlike triple-helical structures [4]. In order to clarify the structure of the individual cinerean thread, X-ray small-angle scattering measurements of dilute aqueous solutions of native polymer were performed. In solution, cinerean should exhibit its natural conformation. In fact we found the typical scattered intensity pattern of long rigid rods, i.e., the scattered intensity $\Delta I(Q)$ decreasing as Q^{-1} within certain limits of the scattering vector modulus $Q = 4\pi\lambda^{-1} \sin\theta$ (λ = X-ray

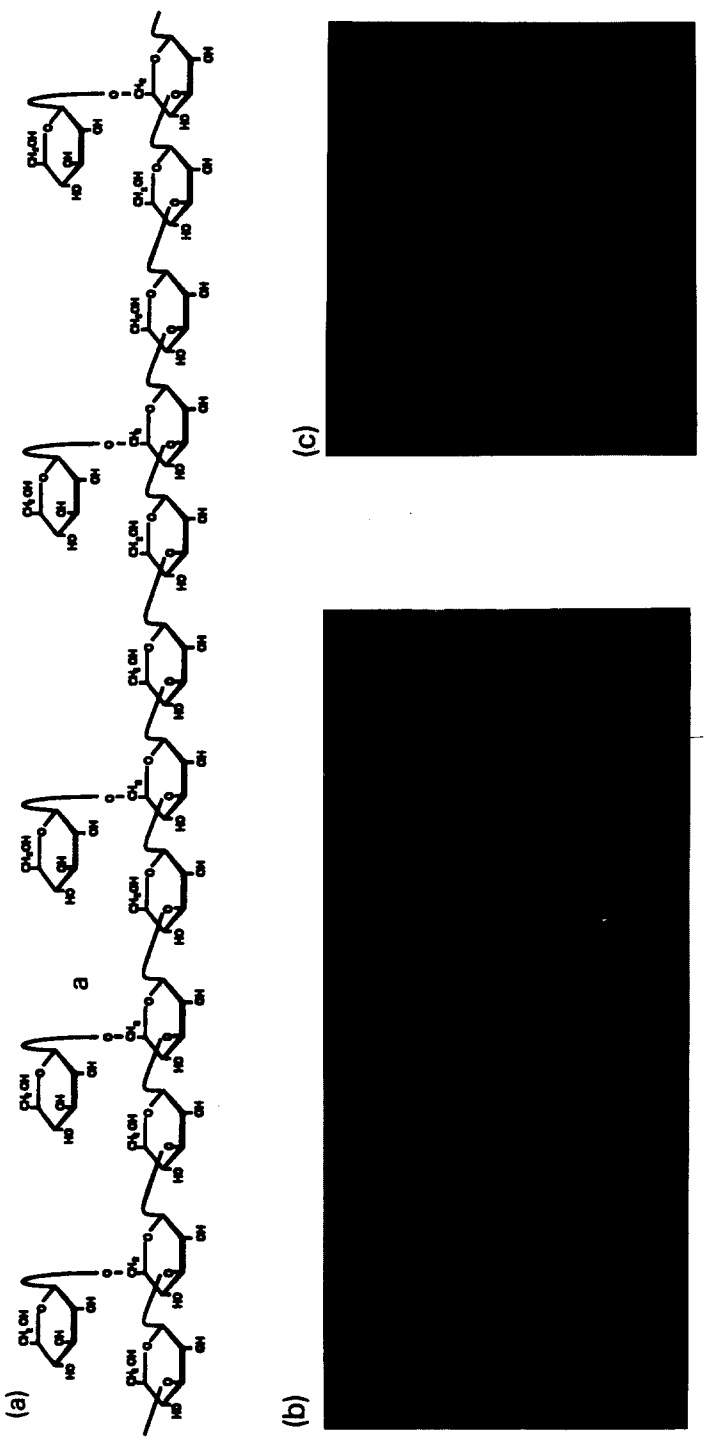

Fig. 1. Statistically branched segment of cinerean. *Botrytis cinerea* produces a β-(1→3)(1→6)-D-glucan named cinerean. The branching degree determined by detection of the products after cleavage of the β-(1→3) linkages was 1.38. (a) Proposed structure in Haworth projection. (b) Ray trace model simulated on a work station by QUANTA. Energy minimization revealed a helical structure stabilized by up to three hydrogen bonds per glycosyl residue; calculated data: mass per unit length = 560 daltons per nm. (c) Sticks model in front view showing the diameter: including branches 1.9 nm, excluding branches 1.1 nm.

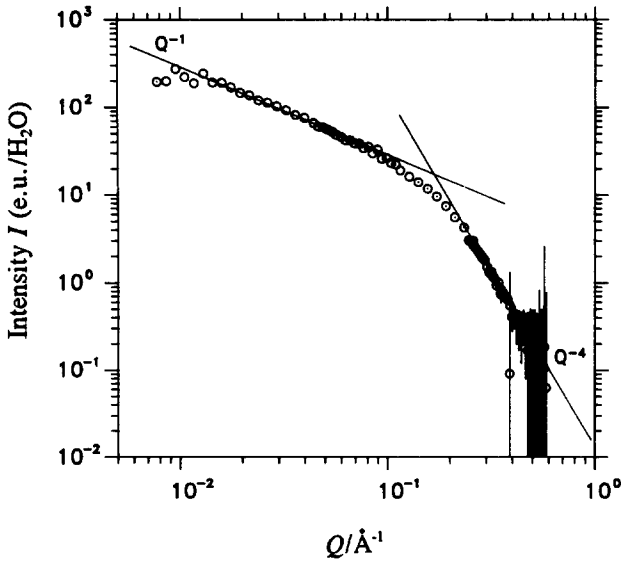

Fig. 2. X-ray small-angle scattering of an aqueous solution of native cinerean.

wavelength, θ = scattering angle). For $Q > 2\pi/L$ (rod length L) the differential scattering cross-section of a single rod is given by [21]

$$\frac{d\sigma}{d\Omega}(Q) = \sigma_{Th}(\Delta\rho)^2 \pi A^2 \frac{L}{Q} \exp(-R^2Q^2/4) \tag{2}$$

where σ_{Th} is the Thomson cross section of the electron, and $\Delta\rho = (M/v) \cdot \Delta z$ the electron density difference (the contrast) with M being the mass of a rod of length L and diameter $2R$ and $v = L \cdot A$ the rod volume; z is the difference in mol-electrons per gram between solute (cinerean) and solvent (water). The intensity $\Delta I(Q)$ scattered from a solution with rod density $n = c \cdot (N_A/M)$ [c = concentration (g/cm^3), N_A = Avogadro's number) into a solid angle element $\Delta\Omega$ is given by $\Delta I(Q) = j_0 F \cdot Dn \, (d\sigma(Q)/d\Omega)\Delta\Omega$, where j_0 is the primary X-ray quantum current density and $F \cdot D$ is the irradiated sample volume. The macroscopic scattering cross-section $(d\Sigma/d\Omega) = n(d\sigma/d\Omega)$ can therefore be written using Eq. 2.

$$\frac{d\Sigma}{d\Omega} = \frac{1}{j_0 F \cdot D} \frac{\Delta I}{\Delta\Omega} = \sigma_{Th} \pi (\Delta z)^2 c N_A \frac{M}{L} \frac{\exp(-Q^2R^2/4)}{Q} \tag{3}$$

An example of a scattering curve is shown in Fig. 2. From Eq. 3 and a calibration run determining the instrumental factor $j_0 F \cdot D$, a rod diameter $2R = 1.9 \pm 0.2$ nm, and a mass per unit length $m_L \equiv M/L = 2250 \pm 490$ daltons/nm were obtained. These data suggest a multiple, most likely helicoidal structure, since a single polymer strand only had a mass per unit length of ca. 560 daltons/nm. The diameter of the single-stranded model taken as the diameter of the enveloping cylinder was found to be ca. 1.9 nm (compare Fig. 1). Although equal to our experimental value for the rod diameter, this is not considered inconsistent with our X-ray results. There is,in fact, sufficient free space left in the single-stranded model to be completed by, for example, two further strands, thus forming a compact rod of equal or nearly equal envelope. For scleroglucan and schizophyllan, which are both described as

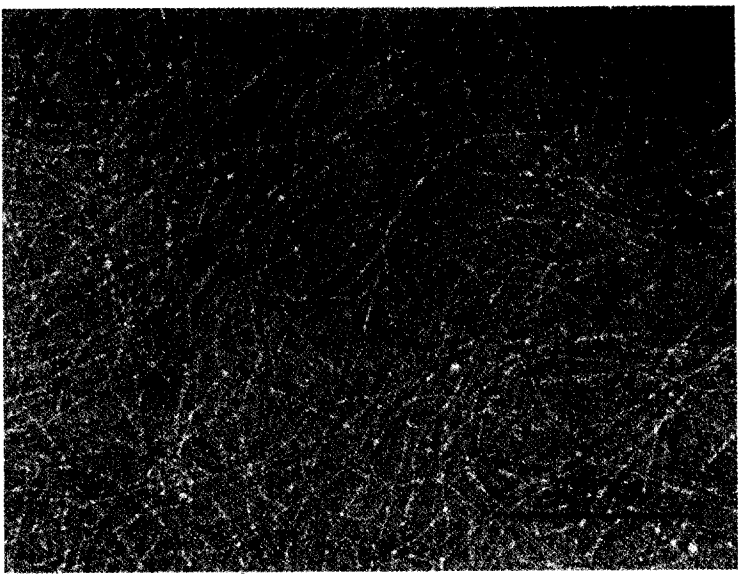

Fig. 3. Electron micrograph of native cinerean negatively stained with uranyl acetate.

triple helices, comparable values for m_L and $2R$ were reported. From light scattering, viscometry, and ultracentrifugation measurements, scleroglucan revealed m_L-values varying between 2050 and 2200 daltons/nm and a rod diameter of 2.4 ± 0.4 nm [4]. For schizophyllan, $m_L = 2170 \pm 50$ nm and $2R = 2.2 \pm 0.6$ were found [22]. Xanthan, a polysaccharide known to form a double-stranded helix, has a mass per unit length of 1940 ± 40 nm as deduced from light scattering experiments [23].

The notion of a rigid, rodlike polymer deduced from the X-ray data could be verified by electron microscopy. Fig. 3 shows an electron micrograph obtained by negative staining with uranyl acetate. The micrograph shows very long cinerean fibrils in random orientations. The network-like appearance is partly due to the preparation method, which started out from a droplet of a dilute cinerean solution placed on the EM grid. Concomitant with the evaporation of the water, the polymer fibrils pile up forming a quasi-two-dimensional random net. The fact that the fibrils are not strictly straight but rather gently curved does not violate the interpretation of the X-ray data as being due to scattering from rigid rods. A scattering technique performs a Fourier analysis of the object imaging spatial dimensions inversely proportional to the scattering vector modulus Q. Satisfying the above condition $Q > 2\pi/L$ guarantees that only sufficiently short and straight portions of the threads are sensed by the X-ray radiation. This is also the reason why only a specific value like "mass per unit length" and not the total mass is determined in this way. (The total mass of a single polysaccharide thread can be measured in the limiting case of zero scattering angle only, provided we have a dilute monodisperse solution.) In other words, both X-ray and electron microscopy data characterize cinerean as a polymer of great persistence length. The persistence length, a, serves as a measure of the rigidity of polymer chains with continuous curvature. It is defined as that chain piece with the mean cosine of the angle ψ between tangents a contour length l_p apart being equal to l/e, that is, $<\cos \psi> = \exp(-l_p/a)$. In an X-ray small-angle scattering curve, the persistence length can be identified with the

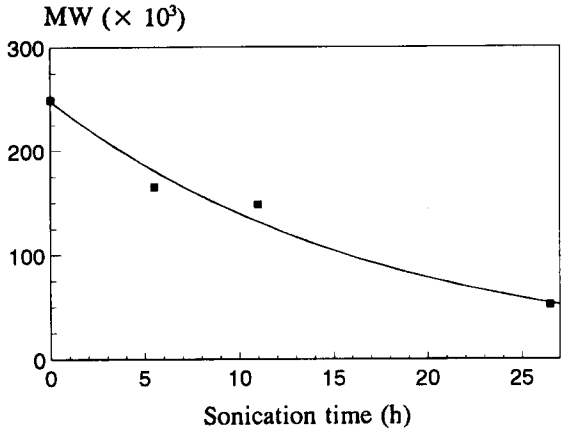

Fig. 4. Time course of cinerean fragmentation by sonication. Average molecular weights were determined by LALLS.

inverse of the smallest Q-value satisfying the Q^{-1}-regime. From the data shown in Fig. 2, a persistence length of $a \approx 300$ nm for cinerean can be estimated. For schizophyllan [22], and xanthan [23], the persistence lengths were found to be 180 ± 30 nm and 120 nm (no error quoted), respectively.

Polymer interactions.—Molecular interaction parameters can be determined by measuring the phase diagram of polymer solutions. According to theory [7], a solution of rigid rods should exhibit a chimney-like two-phase region on top of a miscibility gap. The position as a function of polymer concentration and the width of this narrow region of phase separation, being the fingerprint of rigid rods, depend on the length–diameter ratios x of the solute molecules (compare Fig. 9). The formation of nematic order in solutions or, in other words, the phase separation can be observed by changes in the rheological, optical, or diffraction properties of the solution. With solutions of native cinerean, we did not observe any anomalies or discontinuities in either the viscosity or the turbidity as a function of temperature and polymer concentration. The most obvious reason for this absence is that the native cinerean forms molecules far too long to be considered stiff. This conclusion is supported by our electron microscopy results presented above (Fig. 3), which show fibrils with finite local curvature but unidentifiable ends. Very long semiflexible polymers obviously do not align. They tend rather to form a loose network of physical crosslinks, which give rise to the extremely high viscosity of even very dilute polysaccharide solutions [24].

Cinerean fragmentation.—As one could expect cinerean to be more rigid on a smaller length scale, solutions of native polysaccharide were sonicated in order to obtain shorter chain fragments. We performed a series of fragmentations by varying the duration of sonication. To obtain a size range which is comparable with dextran standards by gel permeation chromatography, a sample with an average molecular weight of 250 000 determined by LALLS was prepared. Starting with this preparation an approximately exponential decrease of $\overline{M}_w$ with the sonication duration down to 50 000 was observed (Table 1 and Fig. 4). In this small range, the decrease in the rate of ultrasonic depolymerization usually observed [25] was rather small. The cinerean fragments obtained were analyzed by gel permeation chromatography. Although the relation $V_e \sim \log M_w$ (V_e = elution volume) only

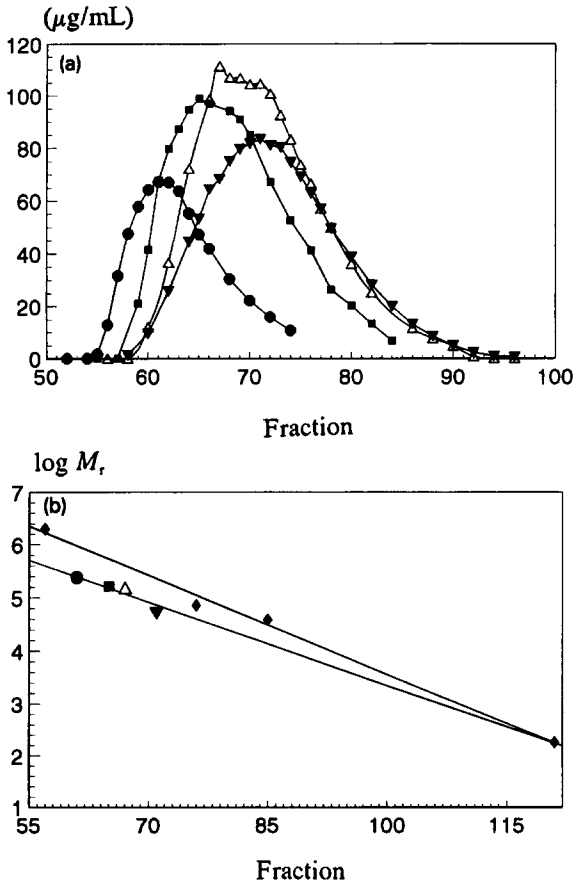

Fig. 5. Gel permeation chromatography (TSK HW 55) of cinerean fragments obtained by sonication. Elution profile (a) and comparison with dextrans and glucose (b). Average molecular weights were determined by LALLS. Cinerean fragments: 249 000 (●), 165 000 (■), 148 000 (▿), and 5200 (▼); dextran standards and glucose (♦): 2 000 000, 72 000, 39 100, 180.

holds for globular particles, the fragments showed this correlation as well (Fig. 5). In comparison with dextran standards the slope was lower, which would lead to an overestimation of the molecular weights. This is consistent with the largely anisometric structure of a rod as compared to a random coil of equal mass. The probability for a rod of given mass, i.e., given length, to be withheld in the pores of the gel is therefore lower.

The molecular mass of fragmented cinerean determined by LALLS represents the weight-average $\overline{M}_W$ of the molecular mass (length) distribution resulting from sonication. The weight-average molecular mass is defined as $\overline{M}_W = \Sigma_i N_i M_i^2 / \Sigma_i N_i M_i$, where N_i is the number of molecules with mass M_i. In order to obtain the detailed mass distribution, we determined both the lengths and numbers of fragmented molecules visualized on some 30 electron micrographs. One of these micrographs of sonicated cinerean is shown in Fig. 6 and the mass distribution is depicted in Fig. 7. From the mass distribution and the known weight-average molecular mass $\overline{M}_W$, the mass per unit length m_L of the fragments is calculated according to

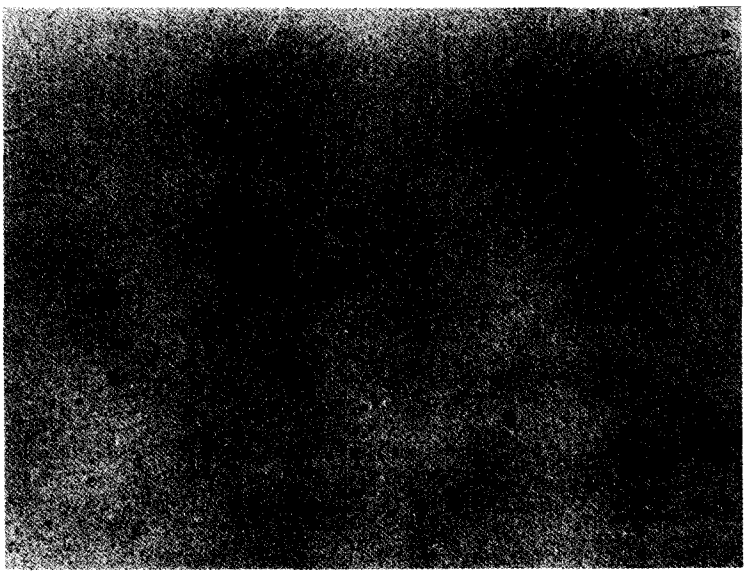

Fig. 6. Electron micrograph of sonicated cinerean freeze-dried and conically coated with platinum.

$$m_L = \overline{M}_W / (\Sigma_i N_i L_i^2 / \Sigma_i N_i L_i) = 1830 \text{ daltons/nm.}$$

This is in reasonable agreement with the value found from our X-ray scattering data on sonicated samples. The topology of the X-ray small-angle scattering curve for sonicated cinerean exhibits the same Q^{-1}- and Q^{-4}-dependences as observed for the native polymer (compare Fig. 2). A separate figure is omitted for that reason. The rodlike shape already demonstrated by electron microscopy (Fig. 6) is therefore confirmed and quantified by the scattering techique. The data evaluation gave a mass per unit length m_L(X-ray) $= 2310 \pm 340$ daltons/nm and a corresponding rod diameter of 1.7 ± 0.3 nm, so both results agree well with those for native cinerean. This was to be expected as neither value need depend on the actual rod length and thereby confirms the data interpretation given for

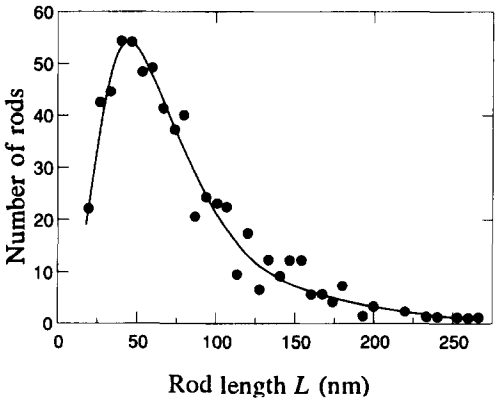

Fig. 7. Length (mass) distribution of a sonicated cinerean sample after 14 h of sonication. Weight-average molecular mass: 172 000 daltons; most probable length: 45 nm; average length: 72 nm.

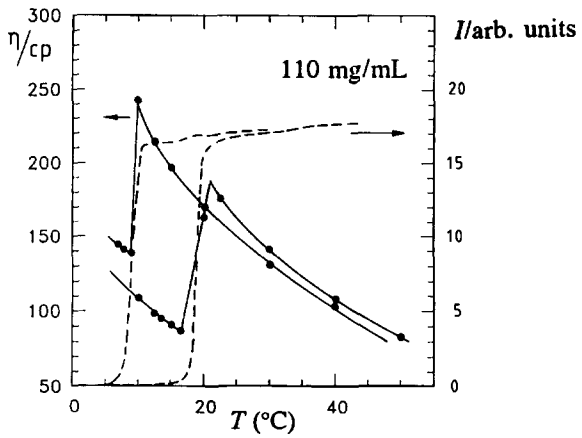

Fig. 8. Typical temperature scan of light transmission (dashed line) and viscosity (solid line through the data points) crossing the phase boundary. The hysteresis is due to the kinetics of the transition. The discontinuities at the lower temperature correspond to the cloud point. The concentration is $c = 0.11$ g/cm^3.

a molecule with finate local curvature. We also deduce that fragmentation does not destroy the assumed triple-helical structure of the native polysaccharide.

Phase diagram determination by nephelometry and rheology.—The fractionated samples readily showed the expected phase separation behavior of solutions of rigid rods, that is, the formation and decay of domains of nematic order within the isotropic solution. This was observed as a reversible turbidity and an accompanying viscosity discontinuity (Fig. 8). An aqueous solution of fractionated cinerean of given concentration and sufficiently high temperature is clear and transparent like pure water. If the temperature is lowered below a certain value (the cloud point), the solution rapidly turns milky. In order to determine the phase transition temperature precisely, we measured the intensity of transmitted laser light as a function of the controlled solution temperature. Raising the temperature of a turbid solution again resulted in a sudden clearing that occurred ca. 10°C above the cloud point. This hysteresis was observed over the entire concentration range investigated.

The viscosity of a solution with no phase separation exhibits a steady viscosity rise with decreasing temperature. On the other hand, the precipitation of anisotropic domains within an isotropic solution on lowering the temperature below a certain value should be accompanied by a corresponding discontinuity of the viscosity. The reason for such behaviour can easily be understood by analogy to ferromagnets: macroscopic anisotropic domains are much more easily aligned by an ordering mechanism (the fluid flow field) than the individual molecules, which are counteracted by thermal agitation.

Measuring the viscosity of the fragmented cinerean solutions as a function of concentration and temperature with a Mikro-Ubbelohde capillary viscosimeter we found the expected discontinuities in viscosity correlated with the cloud and clearing points. A typical temperature scan of both the viscosity and the light transmission is presented in Fig. 8. The phase diagram obtained in this way is shown in Fig. 9. The abscissa is given in units of the normalized volume fraction v_2 of the solute, which corresponds to concentration c (g/cm^3) via the relation $v_2 = c/(c + \rho_{cin})$, where $\rho_{cin} = 1.44$ g/cm^3 is the cinerean density. The reason for the limited v_2-valuesin the experimental phase diagrams is the strongly increasing

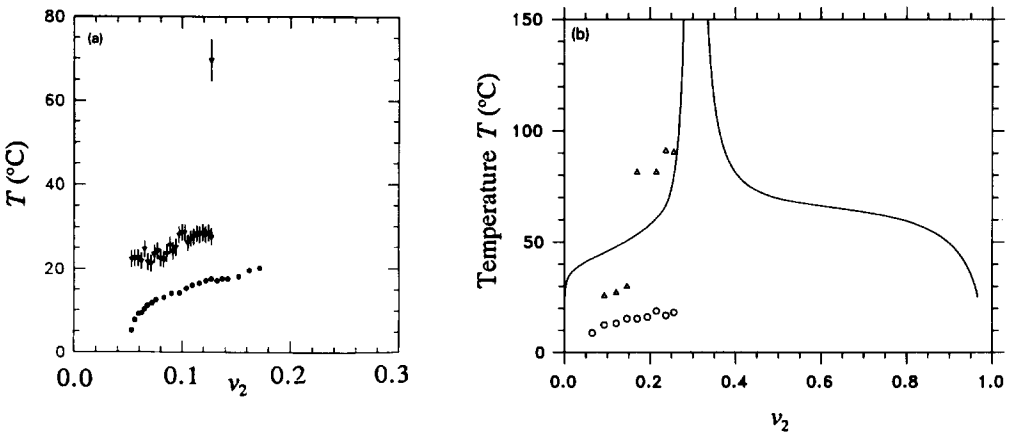

Fig. 9. Phase diagrams for solutions of fractionated cinerean obtained by nephelometry. (a) molecular weight $\overline{M}_w = 198\,000$; cloud point (●), clearing points (▼). (b) Molecular weight $\overline{M}_w = 172\,000$ daltons; cloud point (○), clearing points (▽). solid line: theory after Flory [7] for length–diameter ratio $x = 30$. For definition of v_2 see text.

viscosity with increasing concentration, that is, additional solute material would no longer dissolve homogeneously.

4. Conclusions

We conclude from our X-ray scattering and electron microscopy data that native cinerean forms very long unbranched fibrils of great persistence length. The large persistence length, expressing an extended but not strictly straight conformation, is most likely due to an internal triple-helical structure of the individual cinerean strands. In contrast, fractionated cinerean can be described as consisting of rigid rods which show a characteristic precipitation tendency in aqueous solutions of proper concentration and temperature.

Acknowledgements

We thank Udo Engelbrecht, Peter Hiller, Marlies Hintzen, Wim Pyckhout, Karl-Ludwig Schimz, and Achim Zirkel for technical support and helpful discussions.

References

[1] G. Franz (Ed.), *Polysaccharide*, Springer, Berlin, 1991, pp 124–130.
[2] C. Montant and L. Thomas, *Ann. Sci. Nat. Bot. Veg.*, 18 (1977) 185–192.
[3] K.-P. Stahmann, P. Pielken, K.L. Schimz, and H. Sahm, *Appl. Env. Microbiol.*, 58 (1992) 3347–3354.
[4] T. Yanaki and T. Norisuye, *Polym. J.*, 15 (1983) 389–396.
[5] T. Yanaki, T. Norisuye, and H. Fujita, *Macromolecules*, 13 (1980) 1482–1466.
[6] W.G. Miller, *Ann. Rev. Phys. Chem.*, 29 (1978) 519–535.

[7] P.J. Flory, *Proc. R. Soc. London, Ser. A*, 234 (1956) 73–89.
[8] Q. Ying, B. Chu, R. Qian, J. Bao, J. Zhang, and C. Xu, *Polymers*, 26 (1983) 1401–1407.
[9] J. Blackwell, R.A. Cageao, and A. Biswas, *Macromolecules*, 20 (1987) 667–671.
[10] R.L. Fenichel (Ed.), *Immune Modulation Agents and Their Mechanism*, Deckker, 1984, pp 409–436.
[11] T. Sasaki, N. Takasuka, G. Chihara, and Y.Y. Maeda, *Gann*, 67 (1976) 191–195.
[12] P. Pielken, P. Stahmann, and H. Sahm, *Appl. Microbiol. Biotechnol.*, 33 (1990) 1–6.
[13] K.-P. Stahmann, K.-L. Schimz, and H. Sahm, *J. Gen. Microbiol.*, 139 (1993) 2833–2840.
[14] D. Herbert, P.J. Phipps, and R.E. Strange, *Methods Microbiol.*, 5 (1971) 209–344.
[15] W. Holzmüller and K. Altenburg (Eds.), *Physik der Kunststoffe*, Berlin, 1961.
[16] H.G. Haubold, K. Grünhagen, M. Wagener, H. Jungbluth, H. Heer, A. Pfeil, H. Rongen, G. Brandenberg, R. Möller, J. Matzerath, P. Hiller, and H. Halling, *Rev. Sci. Instrum.*, 60 (1989) 1943–1946.
[17] J.A. Leal, P. Ruperez, and B. Gomez-Miranda, *Trans. Br. Mycol. Soc.*, 72 (1979) 172–176.
[18] D. Dubourdieu and P. Riberau-Gayon, *Carbohydr. Res.*, 93 (1981) 294–299.
[19] O. Kamoen, G. Jamart, H. Declercq, and D. Dubourdieu, *Ann. Phytopathol.*, 12 1980 365–376.
[20] C. Montant and L. Thomas, *Ann. Sci. Nat. Bot. Veg.*, 19 (1978) 39–43.
[21] O. Glatter and O. Kratky (Eds.), *Small Angle X-Ray Scattering*, Academic, New York, 1982.
[22] Y. Kashiwagi, T. Norisuye, and H. Fujita, *Macromolecules*, 14 (1981) 1220–1225.
[23] T. Sato, T. Norisuye, and H. Fujita, *Polym. J.*, 16 (1984) 341–350.
[24] G. Holzwarth, *Dev. Ind. Microbiol.*, 26 (1985) 271–280.
[25] K.S. Suslick (Ed.), *Ultrasound. Its Chemical, Physical, and Biological Effects*, VCH, Weinheim, 1988, pp 150–151.